

# Dalton Transactions

Accepted Manuscript



This is an *Accepted Manuscript*, which has been through the RSC Publishing peer review process and has been accepted for publication.

*Accepted Manuscripts* are published online shortly after acceptance, which is prior to technical editing, formatting and proof reading. This free service from RSC Publishing allows authors to make their results available to the community, in citable form, before publication of the edited article. This *Accepted Manuscript* will be replaced by the edited and formatted *Advance Article* as soon as this is available.

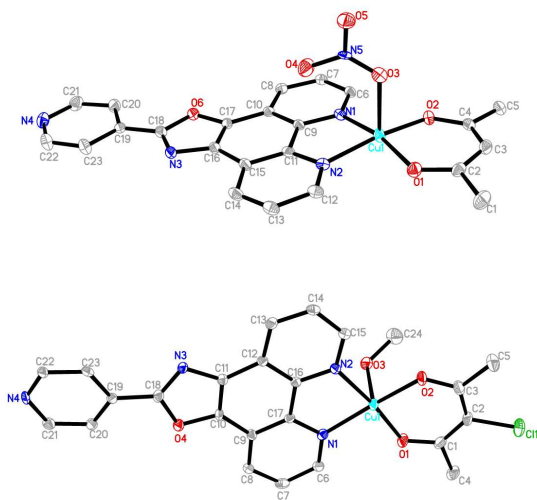
To cite this manuscript please use its permanent Digital Object Identifier (DOI®), which is identical for all formats of publication.

More information about *Accepted Manuscripts* can be found in the [Information for Authors](#).

Please note that technical editing may introduce minor changes to the text and/or graphics contained in the manuscript submitted by the author(s) which may alter content, and that the standard [Terms & Conditions](#) and the [ethical guidelines](#) that apply to the journal are still applicable. In no event shall the RSC be held responsible for any errors or omissions in these *Accepted Manuscript* manuscripts or any consequences arising from the use of any information contained in them.

## Table of Contents

Three new mononuclear copper(II) complexes have been synthesized and characterized. Their interactions with DNA, the nucleolytic cleavage activity and the cytotoxicity were studied.



# Synthesis, characterization, DNA binding, cleavage and cytotoxicity of copper(II) complexes

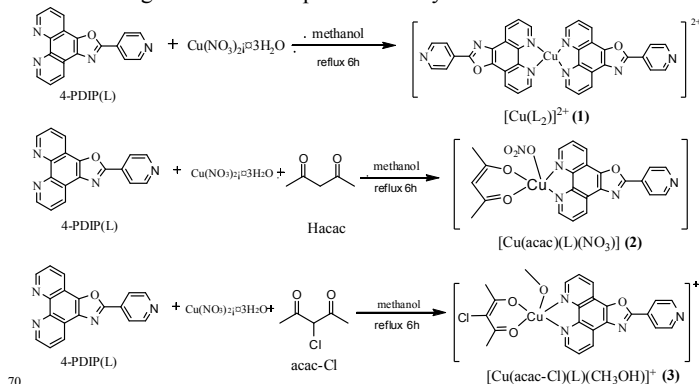
Mei-Jin Li<sup>\*a</sup>, Tao-Yu Lan<sup>a</sup>, Xiu-Hui Cao<sup>a</sup>, Huang-Hao Yang<sup>a</sup>, Yupeng Shi<sup>b</sup>, Changqing Yi<sup>\*b</sup>, Guo-Nan Chen<sup>a</sup>

Three new mononuclear copper(II) complexes  $[\text{Cu}(\text{L}_2)]^{2+}$  (**1**),  $[\text{Cu}(\text{acac})(\text{L})]^+$  (**2**),  $[\text{Cu}(\text{acac}-\text{Cl})(\text{L})]^+$  (**3**), ( $\text{L} = 2$ -(4-pyridine)oxazo[4,5-f]1,10-phenanthroline (4-PDIP); acac = acetylacetonate; acac-Cl = 3-chloroacetylacetonate) have been synthesized and characterized by elemental analysis, high resolution mass spectrometry (Q-TOF), IR spectroscopy. Two of the complexes were structurally characterized by single-crystal X-ray diffraction techniques. Their interactions with DNA were studied by UV-vis absorption and emission spectra, viscosity, thermal melting, DNA unwinding assay and CD spectroscopy. The nucleolytic cleavage activity of the compounds was carried out on double stranded pBR322 circular plasmid DNA by using a gel electrophoresis experiment in the presence and absence of oxidant ( $\text{H}_2\text{O}_2$ ). Active oxygen intermediates such as hydroxyl radicals and hydrogen peroxide generated in the presence of **1** and **3** may act as active species for the DNA scission. The cytotoxicity of the complexes against HepG2 cancer cell was also studied.

## Introduction

DNA cleavage reagents have attracted much attention for their diverse applications such as molecular biology, biotechnology, and medicine.<sup>1-3</sup> Transition metal complexes play an important role in nucleic acids chemistry because of their diverse applications such as footprinting agents, sequence specific binding, structural probes, and therapeutic agents.<sup>4-8</sup> Copper complexes are particularly attractive and extensively studied because of their biologically accessible redox potential and relatively high affinity for nucleobases,<sup>9-11</sup> which are essential to generate reactive oxygen species (ROS) for DNA cleavage in the presence of a reductant and dioxygen.<sup>12,13</sup> Sigman and co-workers have developed the first chemical nuclease  $[\text{Cu}(\text{phen})_2]^+$  and it was proved to have high nucleolytic efficiency in the presence of a reducing agent.<sup>14,15</sup> A series of mononuclear copper(II) polypyridyl and mixed-ligand copper(II) polypyridyl complexes, such as  $[\text{Cu}(\text{dppz})_2\text{Cl}]^{2+}$ ,<sup>16</sup>  $[\text{Cu}(\text{dpq})_2(\text{H}_2\text{O})]^{2+}$ ,<sup>17</sup>  $[\text{Cu}(\text{imda})\text{L}]^{18}$  (where imda = iminodiacetic acid and  $\text{L} = 1,10$ -phenanthroline, 5,6-dimethyl-1,10-phenanthroline, and dipyrido[3,2-d:2',3'-f]quinoxaline), wherein the copper-bound hydroxyl is the active species that hydrolyzes the nucleic acid phosphate backbone have been reported. Recent studies demonstrated that some mononuclear copper(II) complexes can efficiently promote DNA cleavage by selectively oxidizing deoxyribose or nucleobase moieties.<sup>19</sup> Kumbhar and his co-workers<sup>20</sup> have reported efficient DNA cleavage through oxidative route by the complexes  $[\text{Cu}(\text{nip})_2]^{2+}$  and  $[\text{Cu}(\text{nip})(\text{acac})]^+$  (where nip = 2-(naphthalen-1-yl)-1H-imidazo[4,5-f][1,10]phenanthroline), suggesting that the synergy between the metal and ligand resulted in enhancement in DNA cleavage to realize higher efficiency or selectivity.<sup>21-24</sup> Therefore, the design of ligand plays an important role in achieving the selectivity and polypyridyl ligands have received

particular interest for their ability to coordinate metal ions. In present work, we report the complexes of a planar ligand L(4-PDIP) complexation with Cu(II) by forming  $\text{N}_4$  or  $\text{N}_2\text{O}_2$  coordination. The complexes have special structures and electronic properties of diverse chemical reactivity, so that they could combine with DNA through non-covalently binding mode, which is effective and important for them to be anticancer drugs. The synthesis, structural characterization, DNA binding, nuclease activity and cytotoxicity of L (4-PDIP) (L is polypyridyl ligand) and its copper(II) complexes **1-3** (Scheme 1) have been reported. The DNA-compound interactions have been analyzed by means of UV-visible, emission spectroscopy of the DNA-ethidium bromide (EB) system, DNA thermal denaturation, viscosimetric measurements, CD spectroscopy and DNA unwinding assay. The nuclease activity and the ROS species implicated in the DNA cleavage mechanism are all reported. The cytotoxicity of the complexes against HepG2 cancer cell was also studied and they showed a significant antineoplastic activity.



Scheme 1. Synthetic Route for Complexes 1-3.

## Experimental section

### Materials

Copper(II) nitrate trihydrate, 1,10-phenanthroline monohydrate, acetylacetonate, 3-chloroacetylacetonate and ammonium acetate were purchased from Sinopharm Chemical Reagent Co. Ltd. 4-

<sup>a</sup>Key Laboratory of Analysis and Detection Technology for Food Safety (Ministry of Education and Fujian Province), Department of Chemistry, Fuzhou University, Fuzhou 350108, P. R. China. <sup>b</sup>School of Engineering, Sun Yat-Sen University, Guangzhou 510275, P.R. China.

Pyridinecarboxaldehyde was purchased from Alfa Aesar Chemical Reagent Co. Ltd. Calfthymus DNA (CT-DNA) was purchased from Sigma Aldrich Chemical Co. Pvt. Ltd., India.

80 Ethidium bromide (EB) was purchased from Aladin Chemistry Co. Ltd. The supercoiled plasmid pBR322 DNA, proteinase k, and agarose gel were obtained from Sangon (shanghai) Biotechnology Company. E.coli DNA topoisomerase I was obtained from New England Biolabs (Beijing) LTD. Tris-HCl-NaCl buffer solution (TBS, 5 mM Tris, 50 mM NaCl, pH 7.2) for CT-DNA binding experiments. Tris buffer (10 mM Tris-HCl, pH 7.6, and 1 mM EDTA) for the gel-electrophoresis experiments. All reagents were used as received and solvents were purified by the standard methods.

### Synthesis.

1,10-Phenanthroline-5,6-dione was synthesized according to a literature procedure.<sup>25</sup>

#### 2-(4-Pyridine) oxazo[4,5-f]1,10-phenanthroline (4-PDIP) (L).

This compound was synthesized by a literature procedure with minor modifications.<sup>26</sup> A mixture of 4-pyridinecarboxaldehyde (0.212 g, 1 mM), 1,10-phenanthroline-5,6-dione (1.552 g, 20 mM), and ammonium acetate (0.133 g, 1.4 mM) in glacial acetic acid (15 mL) was refluxed for about 4 h under nitrogen atmosphere, then cooled to room temperature and diluted with water (50 mL). The mixture was extracted three times by CH<sub>2</sub>Cl<sub>2</sub>. The combined extracts were dried over anhydrous MgSO<sub>4</sub>, filtered, and evaporated to dryness. The crude product was purified by column chromatography (SiO<sub>2</sub>, CH<sub>2</sub>Cl<sub>2</sub>/MeOH). And pale yellow solid was obtained. Yield 0.15 g, 51%. Positive Q-TOF MS (*m/z*): found 299.0940 (calcd 299.0933). for C<sub>18</sub>H<sub>11</sub>N<sub>4</sub>O ([M+H]<sup>+</sup>). <sup>1</sup>HNMR (400 MHz; CDCl<sub>3</sub>; Me<sub>4</sub>Si): 9.28 (t, *J* = 2 Hz, 2H), 8.97 (dd, *J*<sub>1</sub> = 8 Hz, *J*<sub>2</sub> = 1.6 Hz, 1H), 8.89 (d, *J* = 6 Hz, 2H), 8.73 (dd, *J*<sub>1</sub> = 7.8 Hz, *J*<sub>2</sub> = 1.2 Hz, 1H), 8.23 (d, *J* = 6 Hz, 2H), 7.82 (m, 2H).

[Cu(L<sub>2</sub>)](NO<sub>3</sub>)<sub>2</sub> (I). This complex was prepared by adding a methanolic solution of 4-PDIP (0.050 g, 0.168 mM) to a solution of copper(II) nitrate trihydrate (0.020 g, 0.083 mM) in anhydrous methanol under nitrogen atmosphere, the mixture was heated to reflux for 6 h, and then a large amount of laurel-green precipitate was formed. The mixture was cooled to room temperature, filtered, and washed with small amount of methanol/chloroform followed by diethyl ether. Yield: 0.042 g (65%). Positive Q-TOF MS (*m/z*): found 659.1097 (calcd 659.1005) for C<sub>36</sub>H<sub>20</sub>CuN<sub>8</sub>O<sub>2</sub> ([M-2NO<sub>3</sub>]<sup>+</sup>). IR (KBr pellet, cm<sup>-1</sup>): 1618, 1515, 1380 (C = C, C = N), 552 (Cu-N), 512 (Cu-O). Anal. alcd for C<sub>36</sub>H<sub>20</sub>CuN<sub>10</sub>O<sub>8</sub>·2H<sub>2</sub>O: C, 52.72; H, 2.95; N, 17.08; Found: C, 52.72; H, 2.83; N, 17.20.

[Cu(acac)(L)(NO<sub>3</sub>)] (2). This complex was prepared by adding a methanolic solution of 4-PDIP (0.050 g, 0.168 mM) and acetylacetone (18 μL 0.175 mM) to a solution of copper(II) nitrate trihydrate (0.047 g, 0.168 mM) in anhydrous methanol under nitrogen atmosphere, the mixture was heated to reflux for 6 h. The

solution was cooled to room temperature, and allowed to stand for evaporation at room temperature. After several days, bright green crystals suitable for X-ray crystallography were obtained. Yield: 0.065 g (74 %). Positive Q-TOF MS (*m/z*): found 460.0668 (calcd 460.0597) for C<sub>23</sub>H<sub>17</sub>CuN<sub>4</sub>O<sub>3</sub> ([M-NO<sub>3</sub>]<sup>+</sup>). IR (KBr pellet, cm<sup>-1</sup>): 3068 (ArH), 1579, 1512, 1377 (C = C, C = N), 546 (Cu-N), 512 (Cu-O). Anal. alcd for C<sub>23</sub>H<sub>17</sub>CuN<sub>5</sub>O<sub>6</sub>·4H<sub>2</sub>O: C, 46.43; H, 4.23; N, 11.77; Found: C, 46.44; H, 4.13; N, 11.92.

[Cu(acac-Cl)(L)(MeOH)](NO<sub>3</sub>) (3). This complex was prepared by adding a methanolic solution of 4-PDIP (0.050 g, 0.168 mM) and 3-chloroacetylacetone (0.023 mg, 0.171 mM) to a solution of copper(II) nitrate trihydrate (0.047 g, 0.168 mM) in anhydrous methanol under nitrogen atmosphere, the mixture was heated to reflux for 6 h. The solution was cooled to room temperature, and allowed to stand for evaporation at room temperature to get the fine crystals. Then it was recrystallized again from methanol-acetonitrile solution, after several days, dark green crystals suitable for X-ray crystallography were obtained. Yield: 0.074 g (79%). Positive Q-TOF MS (*m/z*): found 494.0408 (calcd 494.0207) for C<sub>23</sub>H<sub>16</sub>ClCuN<sub>4</sub>O<sub>3</sub> ([M-NO<sub>3</sub>]<sup>+</sup>). IR (KBr pellet, cm<sup>-1</sup>): ν = 3060 (ArH), 1578, 1513, 1451 (C = C, C = N), 552 (Cu-N), 512 (Cu-O). Anal. alcd for C<sub>23</sub>H<sub>16</sub>ClCuN<sub>5</sub>O<sub>6</sub>·H<sub>2</sub>O: C, 48.01; H, 3.15; N, 12.17; Found: C, 48.10; H, 3.22; N, 12.29.

### Methods and instrumentations

<sup>1</sup>H NMR spectra were measured on a BRUKER AVANCE III 300MHz spectrometer. Chemical shifts (ppm) were reported relative to tetramethylsilane (Me<sub>4</sub>Si). Positive Q-TOF mass spectra (MS) were recorded on an Agilent 6520 accurate mass spectrometer. FT-IR spectra were recorded as KBr pellets on a Thermo Fisher FT-IR Nicolet 6700 spectrophotometer. UV-Vis absorption spectra and DNA thermal denaturation experiments were taken on a Lambda 750 spectrophotometer. Emission spectra were carried out on a Hitachi fluorescence F-4600 spectrophotometer (PMT: 700V). Circular dichroism spectra were recorded on an AVIV Model 420 spectropolarimeter. Viscosity measurements were carried out using JC522-1835 Ubbelohde viscometer.

Cyclic voltammetry (CV) was performed with a Model CHI 660 electrochemical analyzer (Shanghai Chenhua Apparatus Company, China), using a three-electrode cell consisting of a 2-mm-diameter GC working electrode (Shanghai Chenhua Apparatus Company, China), a Ag/AgNO<sub>3</sub> reference electrode in DMF and a Pt wire counter electrode. Electrochemical measurements were performed in DMF solutions with 0.1 M <sup>n</sup>Bu<sub>4</sub>NPF<sub>6</sub> as the supporting electrolyte at room temperature.

### Crystal structural determination

Crystal structures of complexes 2 and 3 were obtained by single-crystal X-ray diffraction technique. The crystallographic data collection for complex 2 was carried out on a beam line 3W1A at BSRF (Beijing Synchrotron Radiation Facility) with a mounted MarCCD-165 detector using synchrotron radiation (λ = 0.75 Å) at

T = 103 K. Data reduction and numerical absorption correction were applied with HKL2000 software.<sup>27</sup> The data for complex **3** was collected on SMARTAPEXCCD single-crystal X-ray diffractometer using graphite-monochromated Mo-K $\alpha$  ( $\lambda$  = 0.71073 Å) at T = 173K. An absorption correction by SADABS was applied to the intensity data. The structures were solved by direct methods or Patterson procedure and the heavy atoms were located from E-map. The remaining non-hydrogen atoms were determined from the successive difference Fourier syntheses. All non-hydrogen atoms were refined anisotropically except those mentioned otherwise. The hydrogen atoms of complex **2** were generated geometrically with isotropic thermal parameters. The hydrogen atoms except those of water molecules in complex **3** were generated geometrically and refined isotropically using the riding model. The hydrogen atoms of free water molecules O1w and O2w in the complex **3** were not found. Atoms N3 and O6 in complex **3** were disordered into two positions with site occupancies of 0.89 and 0.11, respectively. Crystal parameters and details of the data collection and refinement are given in Table 1.

**Table 1.** Crystallographic data for the complexes **2** and **3**

Complex	<b>2</b>	<b>3</b>
Empirical formular	C <sub>23</sub> H <sub>17</sub> CuN <sub>5</sub> O <sub>6</sub>	C <sub>24</sub> H <sub>23</sub> ClCuN <sub>6</sub> O <sub>11</sub> (C <sub>23</sub> H <sub>17</sub> ClCuN <sub>4</sub> O <sub>3</sub> ·CH <sub>3</sub> OH·H <sub>2</sub> O·(NO <sub>3</sub> ) <sub>2</sub> )
Formular weight	522.96	670.47
Crystal system	Monoclinic	Triclinic
space group	P2(1)/c	P-1
a/Å	9.4230(19)	8.495(2)
b/Å	24.454(5)	9.358(3)
c/Å	9.2950(19)	17.422(5)
a/deg	90	91.295(6)
$\beta$ /deg	92.63(3)	96.015(6)
$\gamma$ /deg	90	102.204(6)
V/Å <sup>3</sup>	2139.0(7)	1344.8(7)
Z	4	2
$\rho_{\text{calcd}}/\text{g cm}^{-3}$	1.624	1.656
$\mu/\text{mm}^{-1}$	1.242	0.985
Radiation( $\lambda$ , Å)	0.75000	0.71073
F(000)	1068.0	686.0
Temp/K	293(2)	173(2)
Reflections collected	5902	7313
Final R1( $F_o$ ) <sup>a</sup>	0.0383	0.0764
Final wR2( $F_o^2$ ) <sup>b</sup>	0.1154	0.1742
GOF	1.012	1.041

$$^a R1 = \sum |F_o - F_c| / \sum F_o \quad ^b wR2 = \sum [w(F_o^2 - F_c^2)^2] / \sum [w(F_o^2)^2]^{1/2}$$

## DNA binding experiments

Absorption spectral titration experiments were carried out for CT-DNA with the various compounds. The stock solution of CT-DNA was prepared with a buffer (5 mM Tris-HCl/50 mM NaCl, pH 7.2) and stored at 4 °C for complete dissolution. The concentration of CT-DNA was determined by UV absorbance at 260 nm, taking 6600 M<sup>-1</sup>cm<sup>-1</sup> as the molar absorption coefficient. The ratio of the UV absorbance at 260 and 280 nm ( $A_{260}/A_{280}$ ) was ca 1.8, indicating that the DNA solution was sufficiently free of protein.<sup>28</sup>

The competitive binding study was carried out by maintaining the EB (2  $\mu$ M) and CT-DNA (4  $\mu$ M) in DMSO-TBS (V/V, 1/14) solution, and increasing the concentrations of the synthesized L and complexes **1-3**. The fluorescence spectra of a series of solutions with various concentrations of the L, **1-3** (0-60  $\mu$ M) and a constant EB-CT-DNA were measured at room temperature (excitation at 520 nm). The apparent binding constant ( $K_{\text{app}}$ ) has been calculated from the eq 1.<sup>29</sup>

$$K_{\text{EtBr}}[\text{EB}] = K_{\text{app}}[\text{complex}] \quad (1)$$

where  $K_{\text{EtBr}}$  is  $1 \times 10^7 \text{ M}^{-1}$  and the concentration of EB is 2  $\mu$ M; [complex] is the concentration of the complex causing 50% reduction in the emission intensity of EB.

DNA thermal denaturation studies were carried out by monitoring the absorption intensity of CT-DNA (50  $\mu$ M) in 1.6% DMSO-TBS buffer solution (pH 7.2) at 266 nm by varying the temperature from 30 to 95 °C in both the absence and the presence of the different complex with a complex to CT-DNA molar ratio of 1:10.

The viscosity measurements were carried out using an Ubbelohde viscometer immersed in a constant temperature bath at 27.2 °C. The data were presented as  $\eta/\eta_0$  vs [complex]/[DNA], where  $\eta$  is the specific viscosity of DNA in the presence of the complexes and  $\eta_0$  is the specific viscosity of DNA alone in DMSO/TBS (V/V, 1/13) buffer. Specific viscosity values were calculated from the observed flow time of DNA solutions (t) corrected for the buffer alone ( $t_0$ ),  $\eta = (t-t_0)/t_0$ .

Circular dichroism spectroscopy was run on an AVIV Model 420 spectropolarimeter at 2.5 nm/s scanning rate, using 1 mm path quartz cuvettes. In the CD absorption spectrometry, the working solution of each sample was prepared by using  $2 \times 10^{-4}$  M DNA and the compounds were titrated into the DNA solution stepwise with the [DNA]/[compound] ratio ranging from 10:0.5 to 10:5. The working solution was incubated for 5 min after each addition. The CD signals of the TBS were subtracted as the background.

The level of DNA intercalation was studied by an unwinding assay. The supercoiled plasmid pBR322 DNA was incubated with different concentrations of the compounds from a DMSO stock solution into a pH 7.9 reaction buffer containing 50 mM potassium acetate, 20 mM Tris-acetate, 10 mM magnesium

acetate, 1 mM dithiothreitol, and 50  $\mu\text{g}$  of bovine serum albumin at 37  $^{\circ}\text{C}$  for 10 min. And then it was incubated with 0.4  $\mu\text{L}$  E.coli DNA topoisomerase I in storage buffer at 37 $^{\circ}\text{C}$  for 15 min, during which supercoiling in the plasmid without any intercalator was fully and irreversibly relaxed. Subsequently, the mixture was added 0.5  $\mu\text{L}$  proteinase K (300  $\mu\text{g}/\text{mL}$ ) in 20 mM EDTA and 0.1% SDS solution and incubated for an addition 30 min. Reactions were terminated by adding 1 $\mu\text{L}$  10 $\times$ loading buffer (0.05% bromo phenol blue, 50% glycerol, and 0.9% SDS). When the intercalator was removed, the supercoiling of the intercalated portion would be reinstated. The samples were analyzed by 1% agarose gel electrophoresis (Tris-boric acid-EDTA (TBE) buffer, pH = 8.2) for 2.5 h at 55 V. The DNA bands representing the plasmid DNA with different supercoiling remaining (topoisomers) were then visualized with staining with GelRed DNA dye (Biotium, Inc.) under UV light and photographed for analysis.

The DNA cleavage studies were carried out by agarose gel electrophoresis on a 15  $\mu\text{L}$  total sample volume containing pBR322 DNA (100 ng/ $\mu\text{L}$ ) in 5% DMF and 95% Tris buffer (10 mM Tris-HCl, pH 7.6, and 1 mM EDTA). For the gel-electrophoresis experiments, supercoiled pBR322 DNA was treated with different concentrations of the compounds or treated with different concentrations of the compounds and  $\text{H}_2\text{O}_2$  as a reducing agent. The mixtures were incubated in the dark for 30 min at 37  $^{\circ}\text{C}$ , followed by its addition to the loading buffer containing 0.25% bromophenol blue; 0.25% xylene cyanol FF; 60% glycerol (3  $\mu\text{L}$ ). The samples were analyzed by 1% agarose gel electrophoresis (Tris-boric acid-EDTA (TBE) buffer, pH = 8.2) for 3 h at 60 V. The gel was stained with 0.5  $\mu\text{g}/\text{mL}$  ethidium bromide and visualized by UV light and photographed for analysis. The cleavage efficiency was measured by determining the ability of the compounds to convert the supercoiled (SC) DNA to the nicked circular (NC) form and linear circular (LC) form.

For mechanistic investigations, experiments were carried out in the presence of different radical scavenging agents. Scavenging agent, such as DMSO (4.3  $\mu\text{L}$ , 4 mM), potassium iodide (4.3  $\mu\text{L}$ , 4 mM), or sodium azide (4.3  $\mu\text{L}$ , 4 mM) was added respectively to the solution of supercoiled DNA (100 ng/ $\mu\text{L}$ ) prior to the addition of the compounds and  $\text{H}_2\text{O}_2$  in the Tris buffer. The mixture was diluted with the buffer to a total volume of 15  $\mu\text{L}$ . The reaction was initiated, quenched, and analyzed according to the procedures described above.

The MTT assay was used to determine the viability of HepG2 cells upon treatment with L and complexes **1-3**. HepG2 cells were seeded in 96-well tissue culture plates at the density of  $5 \times 10^5$  cells per well and incubated for three days. After treatment with the complexes **1-3** or cisplatin for 24h, the plates were washed twice with culture medium, then MTT was added and the plates were incubated for another 4 h. Cells without any treatment were used as control. The relative cytotoxicity was expressed in percentage of  $[\text{OD}_{\text{sample}} - \text{OD}_{\text{blank}}] / [\text{OD}_{\text{control}} - \text{OD}_{\text{blank}}] \times 100$ .

Data were collected from three independent experiments and expressed as the mean  $\pm$  standard deviation (SD). The statistical differences were analyzed by a paired Student's *t*-test. *P* values less than 0.05 were considered to indicate statistical differences.

## Results and discussion

### Synthesis and characterization

The ligand L was prepared by reaction of 1,10-phenanthroline-5,6-dione and 4-pyridylcarbinol in the presence of ammonium acetate in glacial acetic acid. It should be noted that an oxazo ligand was achieved in our experiment instead of imidazo ligand. It was confirmed by high resolution mass spectrometry (Q-TOF) and  $^1\text{H}$ NMR. The corresponding copper(II) complexes were synthesized in good yield and characterized by ESI-MS, elemental analysis, UV-visible, emission and FT-IR spectroscopy. The compounds **2** and **3** were also characterized by the single crystal X-ray structure.

### Crystal structures

Single crystals of complexes **2** and **3** suitable for X-ray diffraction were grown by slow evaporation of the methanol of compounds at room temperature. The solid state structures of **2** and **3** have been determined by X-ray crystallography and ORTEP drawings of **2** and **3** depicted in Figure 1. The monoclinic crystal system of complex **2** is belonging to the P21/c space group with metal in a 4+1 square-pyramidal  $\text{CuN}_2\text{O}_3$  coordination geometry in which the apical site is occupied by a nitrate ion. The triclinic crystal system of complex **3** is belonging to the space group P-1 with metal in a 4+1 square-pyramidal  $\text{CuN}_2\text{O}_3$  coordination geometry, the apical site is occupied by a coordinated methanol molecule. The donor atoms in each basal plane are two nitrogen atoms from the polypyridyl ligand and two ortho oxygen atoms of the acac ligand. The apical site has a nitrate ion with a Cu1-O3 distance of 2.214  $\text{\AA}$  for the complex **2** and a coordinate methanol molecule with a Cu1-O3 distance of 2.348  $\text{\AA}$  for the complex **3** compared to the equatorial Cu-O (1.93-1.99  $\text{\AA}$ ). Selected bond lengths and angles for the molecules of **2** and **3** were listed in Table 2.

**Table 2.** Selected bond distances ( $\text{\AA}$ ) and angles ( $^{\circ}$ ) for the complexes **2** and **3**

Complex 2		Complex 3	
Cu(1)-O(1)	1.924(2)	Cu(1)-O(2)	1.907(4)
Cu(1)-O(2)	1.925(2)	Cu(1)-O(1)	1.909(4)
Cu(1)-N(1)	2.020(2)	Cu(1)-N(1)	2.011(5)
Cu(1)-N(2)	2.012(2)	Cu(1)-N(2)	2.015(4)
Cu(1)-O(3)	2.214(2)	Cu(1)-O(3)	2.348(4)
O(1)-Cu(1)-O(2)	94.19(8)	O(2)-Cu(1)-O(1)	93.47(2)
O(1)-Cu(1)-N(1)	167.73(9)	O(2)-Cu(1)-N(1)	167.90(2)
O(2)-Cu(1)-N(1)	91.19(8)	O(1)-Cu(1)-N(1)	91.56(2)
O(1)-Cu(1)-N(2)	90.31(8)	O(2)-Cu(1)-N(2)	92.47(2)
O(2)-Cu(1)-N(2)	166.03(8)	O(1)-Cu(1)-N(2)	173.63(2)
N(1)-Cu(1)-N(2)	82.01(8)	N(1)-Cu(1)-N(2)	82.17(2)
O(1)-Cu(1)-O(3)	90.80(8)	O(2)-Cu(1)-O(3)	95.48(2)
O(2)-Cu(1)-O(3)	94.61(8)	O(1)-Cu(1)-O(3)	90.64(2)
N(1)-Cu(1)-O(3)	99.76(8)	N(1)-Cu(1)-O(3)	95.45(2)
N(2)-Cu(1)-O(3)	98.55(8)	N(2)-Cu(1)-O(3)	91.09(2)

355

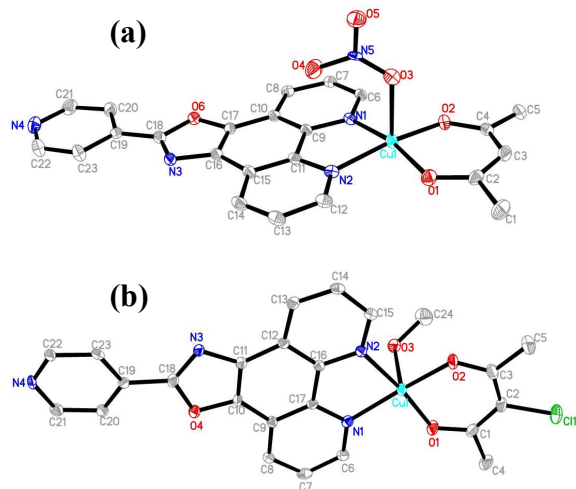


**Figure 1.** ORTEP drawing of the complexes **2** (a) and **3** (b) with atom labeling scheme showing 30% thermal ellipsoids.

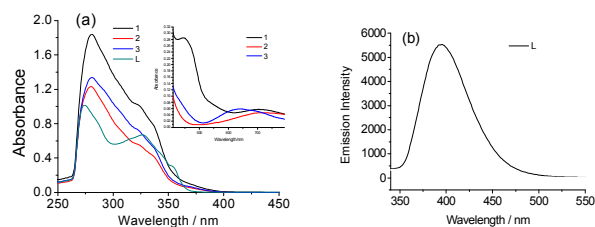
### 360 Photophysical studies

The photophysical properties of **L** and complexes **1-3** are summarized in Table 3. The absorption properties of the complexes **1-3** in DMSO solution were shown in Figure 2a. The bands between 260 and 400 nm were attributed to  $\pi$  to  $\pi^*$  transitions of the aromatic nitrogen donor ligands. The low-energy bands around 450 nm for complex **1** assigned as the  $(d\pi(\text{Cu})) \rightarrow \text{ligand} (\pi^*(\text{N-N}))$ , and the bands around 640-709 nm for complexes **1-3** are all assigned as metal d-d transitions typical of copper(II) complexes.<sup>31</sup> The stability properties of **L**, complexes **1-3** were tested from 0.5-24 h in DMSO and 5% DMSO-TBS solution at room temperature, respectively. There were very small changes in the UV-vis spectra of these complexes with a less than 5% decreasing of the absorbance at about 280 nm, which showed that the complexes were stable in DMSO or DMSO-TBS solution.

375 The excitation at ca. 320 nm of **L** in DMSO at room temperature results in an intense emission peak centered at 395 nm (Figure 2b). The complexes **1-3** were non-emissive as most Cu(II) complexes,<sup>32</sup> because Cu(II) was well-known to quench ligands' emission. A very weak emission centered at 395 nm same to ligand was observed for complexes **1-3**, which was probably due to ligand scrambling.

**Table 3.** Photophysical data for **L** and complexes **1-3**

Compound	Absorption $\lambda_{\text{max}}/\text{nm}$ $\epsilon / \text{dm}^3\text{mol}^{-1}\text{cm}^{-1}$
<b>L</b>	274(29470), 326(18627), 353(8685)
<b>1</b>	280(68263), 322(51160), 445(285.1), 702(57.3)
<b>2</b>	279(50185), 323(28093), 709(46.9)
<b>3</b>	280(55278), 325(30323), 640(58.6)



385

**Figure 2.** (a) UV-visible spectra of **L**, **1-3** (20  $\mu\text{M}$ ) in DMSO; the inset shows UV-visible spectra of complexes **1-3** (1 mM) in DMSO. (b) Emission spectra of **L** (2  $\mu\text{M}$ ).

### 390 Electrochemistry

Cyclic voltammetry of complexes **1-3** was performed with a glassy carbon electrode at a scan rate of 0.1 V/s in DMF containing  ${}^n\text{Bu}_4\text{NPF}_6$  (0.1 M) as supporting electrolyte. The complexes are redox active and show a quasireversible cyclic voltammetric response at -0.31 V vs. Ag/AgNO<sub>3</sub> ( $\Delta E_p = 180$  mV) for complex **1**, an irreversible peak at for -0.81 V, -0.77 V vs. Ag/AgNO<sub>3</sub> for complexes **2** and **3**, respectively. The redox peaks were assigned to the  $\text{Cu}^{\text{II}}/\text{Cu}^{\text{I}}$  couple and the redox potential of the complexes was accessible for nucleobases.<sup>9, 33</sup> The cyclic voltammogram of complex **1** is shown in Figure 3, and the cyclic voltammograms of complexes **2** and **3** are shown in supporting information (Fig S5). The redox potential of complex **1** was relatively higher than that of complexes **2** and **3**, which was attributed to the extension of the corresponding  $\pi$  frame-work around the metal centre.<sup>16</sup>

405

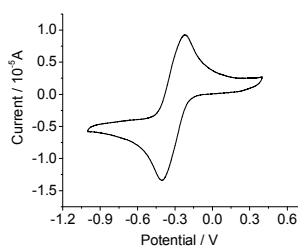


**Figure 3.** Cyclic voltammogram of complex **1** in DMF (0.1 M  ${}^n\text{Bu}_4\text{N PF}_6$ ) on a GC working electrode. Scan rate: 0.1  $\text{Vs}^{-1}$ .

### 410 Absorption spectra studies of CT-DNA binding with **L** and the complexes

Electronic absorption spectra of **L** and **1-3** were carried out to test the bonding ability with CT-DNA. Upon addition of DNA to the solution of **L**, the peak at 274 nm increased obviously due to the absorbance of the DNA, while a very slight decrease was observed at the absorption peak 326 nm. With the increasing concentration of DNA added to the solution of **1-3**, there was some decrease in the intensity and a hypochromism at the range of 290-350 nm, which suggested that there was a higher affinity toward DNA for **1-3** than **L**, as shown in Figure 4. It was explained that a complex binding to DNA through intercalation usually resulted in hypochromism and bathochromism, which

420

involved strong stacking interaction between an aromatic chromophore and the base pairs of DNA.<sup>34</sup>

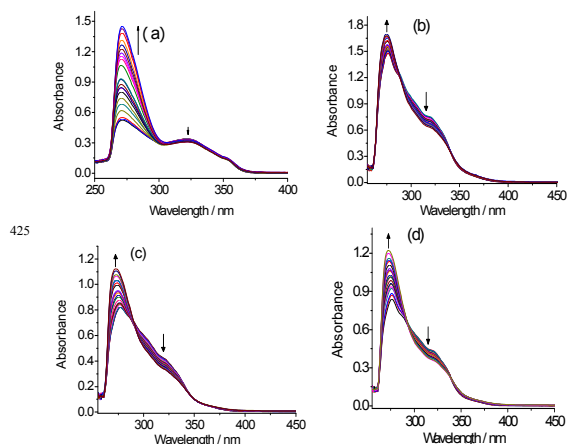


**Figure 4.** Absorption spectra of L and complexes **1-3** (20  $\mu\text{M}$ ) upon the titration of CT-DNA (0-80  $\mu\text{M}$ ) in 6.6 % DMSO-TBS solution, respectively.

#### Ethidium bromide displacement assay for DNA binding

Ethidium bromide (EB) is a standard intercalating agent of DNA. A competitive binding study using ethidium bromide (EB) bound to DNA was carried out by successive addition of 0-60  $\mu\text{M}$  of each compound to EB-DNA system in DMSO-TBS (V/V: 1/14) solution. The emission spectra of EB-DNA system in the presence and absence of each compound are shown in Figure 5.

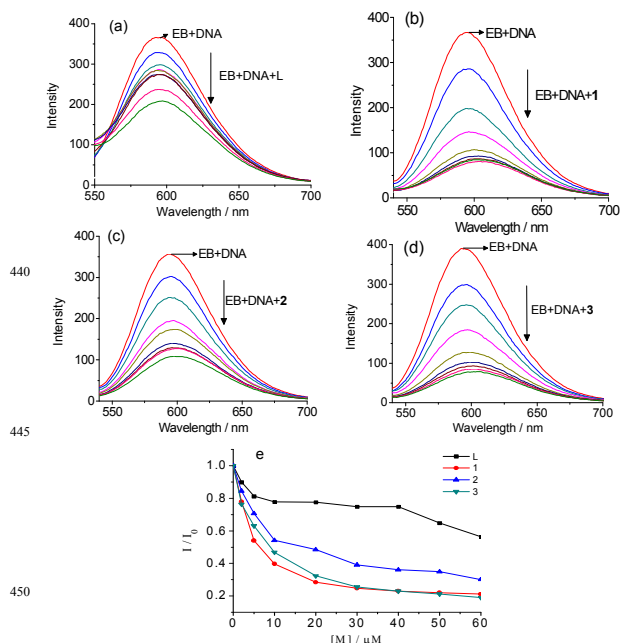


**Figure 5.** (a-d) Effect of L and **1-3** (0-60  $\mu\text{M}$ ) on the emission intensity of the CT-DNA (4  $\mu\text{M}$ )-bound ethidium bromide (2  $\mu\text{M}$ ) at different concentrations in DMSO-TBS (V/V, 1/14) solution. (e) Plots of relative integrated emission intensity versus  $[\text{DNA}]/[\text{M}]$  for L and **1-3**.

After addition of the compound to the EB-DNA system, the emission was quenched by about 43 %, 78 %, 70 % and 80 % for L and complexes **1-3**, respectively. The results showed that the compounds would efficiently compete with EB for intercalative binding sites on DNA by replacing EB, especially for **1**. According to equation 1,<sup>29</sup>  $K_{\text{app}}$  values are evaluated as  $2.0 \times 10^5$ ,  $4.0 \times 10^6$ ,  $2.0 \times 10^6$ ,  $2.7 \times 10^6 \text{ M}^{-1}$  for L and complexes **1-3**, respectively. The values were less than the binding constant of the classical intercalators and metallointercalators ( $10^7 \text{ M}^{-1}$ ), especially for L, which suggested that the interaction between the planar aromatic L and DNA was a moderate intercalative mode. The higher values of  $K_{\text{app}}$  for the complexes **1-3** indicated of the stronger binding ability toward DNA than L, which was consistent with the UV-vis spectral titration results. It seems that combing L with Cu(II) ion would reinforce its binding to CT-DNA and the copper(II) ion plays important roles in the high cytotoxicity of the copper(II) complexes.

#### DNA melting studies

The melting temperature ( $T_m$ ) of DNA characterizes the transition from double-stranded to single-stranded nucleic acid.<sup>35</sup> The experiment was tested in the absence and presence of L, and the complexes **1-3** at different temperature, which is shown in Figure 6. This experiment could give insight into their conformational changes and information about the interaction strength with DNA in the presence of the compound. The melting temperature ( $T_m$ ) of CT-DNA was found to be 76  $^\circ\text{C}$ . In the presence of L and **1-3**,  $T_m$  of CT-DNA was raised to 80, 83, 82 and 81  $^\circ\text{C}$ , respectively, by an increase of melting temperature ( $\Delta T_m$ ) about  $\sim 4-7 \text{ }^\circ\text{C}$ . The results suggested that the compounds were involved in the stabilization of duplex DNA and the complexes were stronger binders to duplex DNA than L.

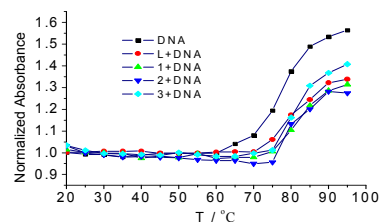


**Figure 6.** Thermal denaturation graph of CT-DNA (50  $\mu\text{M}$ ) in the absence and presence of L, **1**, **2** and **3** (5  $\mu\text{M}$ ).

#### Viscosity experiments

To further investigate the binding nature of the complexes with DNA, viscosity measurements on the solutions of DNA incubated with the compounds have been carried out. The viscosity of CT-DNA solution increased after addition of the solution of L, **1-3** and EB. With  $C_M/C_{\text{DNA}}$  of L, the complexes **1-3** and EB increasing, the viscosity of the CT-DNA increased, as shown in Figure 7. Intercalation of a species into DNA base pairs generally caused a significant increase in the viscosity of the DNA solution,



due to an increase in the separation of the base pairs to accommodate the bound species, which was evidenced by a classical DNA intercalator like EB.<sup>36, 37</sup> And nonclassical intercalation under the same conditions typically caused either a less pronounced change (positive or negative) in DNA solution viscosity or none at all.<sup>38</sup> The changes of the relative viscosity of CT-DNA bound to the complexes were similar to the known intercalator EB. There was a relatively small increase in the viscosity of DNA for L compared to complexes 1-3 and the classical intercalator EB, which indicates a moderate intercalative binding of L to DNA. The increase of the relative viscosity of CT-DNA followed the order, 1>3>2>L (Figure 7). These results parallel the phenomena observed in the competitive binding studies.

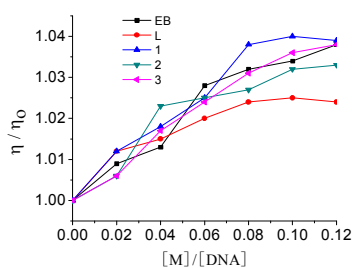


**Figure 7.** Relative viscosity increments of CT-DNA (200 μM) solution bound with L, 1, 2 and 3 with increasing  $C_M/C_{DNA}$  (0.01-0.12).

### DNA unwinding assay

To further confirm the intercalative interaction between the compounds and CT-DNA, a well-established unwinding DNA assay was carried out.<sup>39</sup> The plasmid pBR322 DNA molecules were relaxed with DNA topoisomerase I in the absence and presence of intercalator. Then the plasmid DNA was analyzed for their superhelicity remaining in the population by agarose gel electrophoresis. Supercoiled (SC) plasmid DNA was incubated with different concentrations of the compounds from 1 to 400 μM for 10 min, then relaxed by DNA topoisomerase I and separated in agarose gel. As shown in Figure 8, supercoiled DNA moved fast in the gel (lane 1) in the absence of topoisomerase I, and the supercoiled DNA without intercalator 3 was fully relaxed (RLX) in the topoisomerase I and moved slowly in the gel (lane 2). The more supercoiled or intercalated DNA molecules migrated

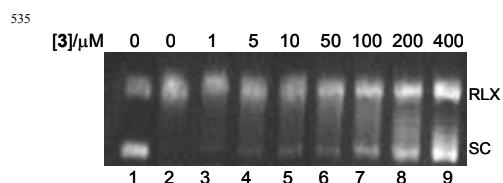


**Figure 8.** Complex 3 intercalated into supercoiled plasmid DNA. Lane 1, SC plasmid DNA without any treatment; lanes 2-9, SC plasmid DNA incubated with increasing concentration of 3 (from 0 to 400 μM).

much faster as increasing the concentration of intercalator (lane 7,8,9). The results for L, 1 and 2 were similar to 3 and shown in the supporting information (Figure S6).

### Circular dichroism spectral analysis of L and the complexes 1-3

Circular dichroism (CD) was used to assess whether nucleic acids undergo conformational changes as a result of complex formation or changes in environment.<sup>40</sup> In the CD spectra, CT-DNA exhibits a positive band at ~278 nm due to base stacking and a negative band at ~245 nm due to the right-handed helicity, which is characteristic of B-DNA.<sup>41</sup> The CD spectrum of DNA was very sensitive to its conformational changes. The addition of L to the solution of CT-DNA induced a decrease in intensity for the negative ellipticity band ~245 nm and an increase in intensity for the positive band at ~278 nm and negative band at ~295 nm with a small blue shift of about 12 nm (Figure 9a), suggesting that the stacking mode and the orientation of base pairs in DNA were disturbed. The phenomenon for complex 1 was similar to L at ~245 and 278 nm bands, while a much larger enhancement in intensity for the negative band at ~295 nm and a new small positive band at ~335 nm were observed as shown in Figure 9b. Since such band and the shift of the main positive band toward shorter waves were characteristic for Z-DNA, it may mean that the DNA strands were locally converted into Z-DNA forms.<sup>42</sup> For complexes 2 and 3, there were a decrease in intensity for the negative ellipticity band at ~245 nm and an increase in intensity for positive band at ~278 nm without shift in the band positions, while the negative band at ~295 nm decreased with the addition of 2 and 3 to the solution of CT-DNA (Figure 9c and 9d). This showed that the CT-DNA would interact with these complexes and might be transformed into other conformations.<sup>43</sup>

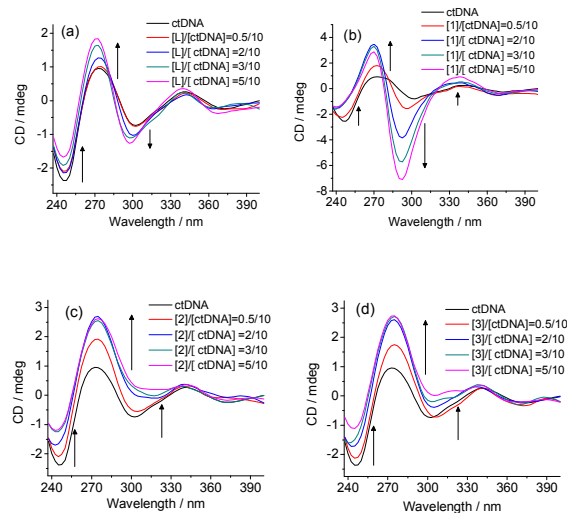


**Figure 9.** CD spectra of CT-DNA (200 μM) in the presence of L(a), the complexes 1 (b), 2(c), 3(d) (0-100 μM) in TBS buffer at room temperature.

### Chemical nuclease activity

To assess the DNA cleavage ability of L and complexes 1-3, supercoiled (SC) pBR322 DNA (100 ng/μL) was incubated with different concentrations of the compounds in 5% DMF in TBE buffer at pH 8.2 for 30 min without the addition of an activator. Upon gel electrophoresis, all of them were cleavage inactive (Figure S7). However, when SC pBR322 DNA (100 ng/μL) mixed with different concentrations of the compounds in 5% DMF in TBE buffer at pH 8.2 for 30 min using H<sub>2</sub>O<sub>2</sub> as an activator (Figure 10), DNA was converted from SC to nicked circular (NC) DNA with increasing concentrations of the compounds. The amounts of SC DNA decreased whereas those of NC DNA increased with increasing concentrations of the compounds and direct double-strand DNA cleavage was not observed in this case. Control experiment showed that copper salts CuNO<sub>3</sub>·3H<sub>2</sub>O were cleavage inactive.

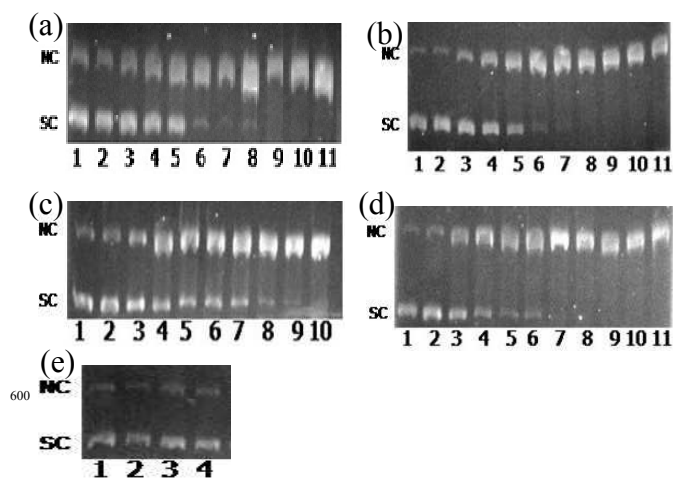


**Figure 10.** (a) Ethidium bromide stained agarose gel (1.0%) of pBR322 plasmid DNA (100 ng/μL) in the presence of L after 30 minutes of incubation with H<sub>2</sub>O<sub>2</sub> (0.4 mM): lane 1, DNA control; lane 2, DNA + H<sub>2</sub>O<sub>2</sub>; lane 3-11, DNA + H<sub>2</sub>O<sub>2</sub> + L (5, 10, 15, 20, 25, 30, 35, 40, 45 μM). (b) Ethidium bromide stained agarose gel (1.0%) of pBR322 plasmid DNA (100 ng/μL) in the presence of complex 1 after 30 minutes of incubation with H<sub>2</sub>O<sub>2</sub> (0.4 mM): lane 1, DNA control; lane 2, DNA + H<sub>2</sub>O<sub>2</sub>; lane 3-11, DNA + H<sub>2</sub>O<sub>2</sub> + 1 (1, 2.5, 5, 7.5, 10, 12.5, 15, 17.5, 20 μM). (c) Ethidium bromide stained agarose gel (1.0%) of pBR322 plasmid DNA (100 ng/μL) in the presence of complex 2 after 30 minutes of incubation with H<sub>2</sub>O<sub>2</sub> (0.4 mM): lane 1, DNA control; lane 2, DNA + H<sub>2</sub>O<sub>2</sub>; lane 3-10, DNA + H<sub>2</sub>O<sub>2</sub> + 2 (5, 10, 15, 20, 25, 30, 35, 40 μM). (d) Ethidium bromide stained agarose gel (1.0%) of pBR322 plasmid DNA (100 ng/μL) in the presence of complex 3 after 30 minutes of incubation with H<sub>2</sub>O<sub>2</sub> (0.4 mM): lane 1, DNA control; lane 2, DNA + H<sub>2</sub>O<sub>2</sub>; lane 3-11, DNA + H<sub>2</sub>O<sub>2</sub> + 3 (1, 2.5, 5, 7.5, 10, 12.5, 15, 17.5, 20 μM). (e) Ethidium bromide stained agarose gel (1.0%) of pBR322 plasmid DNA (100 ng/μL) in the presence of CuNO<sub>3</sub>·3H<sub>2</sub>O after 30 minutes of incubation with H<sub>2</sub>O<sub>2</sub> (0.4 mM): lane 1, DNA control; lane 2, DNA + H<sub>2</sub>O<sub>2</sub>; lane 3, DNA + CuNO<sub>3</sub>·3H<sub>2</sub>O (45 μM); lane 4, DNA + H<sub>2</sub>O<sub>2</sub> + CuNO<sub>3</sub>·3H<sub>2</sub>O (45 μM).

#### Investigation of DNA cleavage in presence of activator and radical scavengers

The involvement of ROS (reactive oxygen species) (hydroxyl, superoxide, singlet oxygen-like species, hydrogen peroxide) in the nuclease mechanism can be inferred by monitoring the quenching of the DNA cleavage in the presence of ROS scavengers in solution. The experiments were carried out in presence of different common scavengers such as DMSO, KI, and NaN<sub>3</sub> (Figure 11). The cleavage activity of L, and complexes 1-3 was reduced dramatically by the presence of hydroxyl radical scavenger DMSO (lanes a7, b2, b6, and c2), indicating that diffusible •OH played a key role in the cleavage process. Hydrogen peroxide scavenger KI also markedly inhibited the cleavage activity of the compounds (lanes a8, b3, b7, and c3), suggesting that H<sub>2</sub>O<sub>2</sub> was involved in the cleavage reaction. Singlet oxygen scavenger NaN<sub>3</sub> did not show inhibition of DNA cleavage (lanes a9, b4, b8, and c4), suggesting that <sup>1</sup>O<sub>2</sub> did not take part in the cleavage mechanism. Therefore, these complexes seemed to follow some similar pathways in the cleavage process, in which hydroxyl radicals and hydrogen peroxide were crucial ROS for the cleavage reactions.

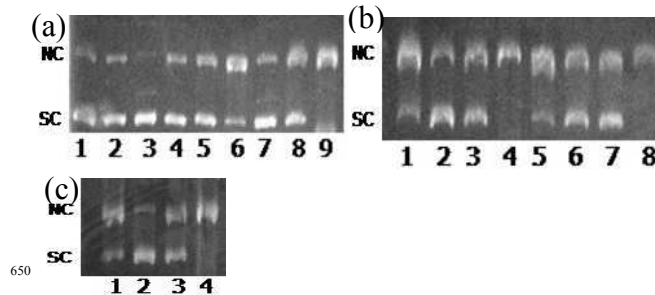


**Figure 11.** (a) Ethidium bromide stained agarose gel (1.0%) of pBR322 plasmid DNA (100 ng/μL) after 30 minutes of incubation with complex 1 (10 μM) and H<sub>2</sub>O<sub>2</sub> in the absence or presence of different scavengers: lane 1, DNA control; lane 2, DNA + H<sub>2</sub>O<sub>2</sub>; lane 3, DNA + H<sub>2</sub>O<sub>2</sub> + DMSO; lane 4, DNA + H<sub>2</sub>O<sub>2</sub> + KI; lane 5, DNA + H<sub>2</sub>O<sub>2</sub> + NaN<sub>3</sub>; lane 6, DNA + H<sub>2</sub>O<sub>2</sub> + 1; lane 7, DNA + H<sub>2</sub>O<sub>2</sub> + 1 + DMSO; lane 8, DNA + H<sub>2</sub>O<sub>2</sub> + 1 + KI; lane 9, DNA + H<sub>2</sub>O<sub>2</sub> + 1 + NaN<sub>3</sub>. (b) Ethidium bromide stained agarose gel (1.0%) of pBR322 plasmid DNA (100 ng/μL) after 30 minutes of incubation with complex 2 (35 μM) and 3 (15 μM) and H<sub>2</sub>O<sub>2</sub> in the absence or presence of different scavengers: lane 1, DNA + H<sub>2</sub>O<sub>2</sub> + 2; lane 2, DNA + H<sub>2</sub>O<sub>2</sub> + 2 + DMSO; lane 3, DNA + H<sub>2</sub>O<sub>2</sub> + 2 + KI; lane 4, DNA + H<sub>2</sub>O<sub>2</sub> + 2 + NaN<sub>3</sub>; lane 5, DNA + H<sub>2</sub>O<sub>2</sub> + 3; lane 6, DNA + H<sub>2</sub>O<sub>2</sub> + 3 + DMSO; lane 7, DNA + H<sub>2</sub>O<sub>2</sub> + 3 + KI; lane 8, DNA + H<sub>2</sub>O<sub>2</sub> + 3 + NaN<sub>3</sub>. (c) Ethidium bromide stained agarose gel (1.0%) of pBR322 plasmid DNA (100 ng/μL) after 30 minutes of incubation with complex L (35 μM) H<sub>2</sub>O<sub>2</sub> in the absence or presence of different scavengers: lane 1, DNA + H<sub>2</sub>O<sub>2</sub> + L; lane 2, DNA + H<sub>2</sub>O<sub>2</sub> + L + DMSO; lane 3, DNA + H<sub>2</sub>O<sub>2</sub> + L + KI; lane 4, DNA + H<sub>2</sub>O<sub>2</sub> + L + NaN<sub>3</sub>.

#### Study of cytotoxicity by MTT Assay

MTT assay was performed to check the antineoplastic effect of L and complexes 1-3. It is found that complexes 1-3 showed significant antineoplastic activities, and their effects on the cellular viability were evaluated in Figure 12. The treatment of HepG2 cells with a series of dilutions (0.1, 0.5, 5, 10 and 20 μM) of L and the new copper(II) complexes resulted in a decrease in

cell viability. L decreases the cell viability by 47% in 24 h at highest dosage (20  $\mu\text{M}$ ), while complexes **1-3** decreased the cell viability by 90%, 89% and 87% in at highest dosage (20  $\mu\text{M}$ ), respectively. The cytotoxicity of the compounds by the IC50 value was 21.2, 3.6, 3.9 and 4.2  $\mu\text{M}$  for L and **1-3** (Table 4), respectively. On comparison of the IC50 value of complexes **1-3** with cisplatin against HepG2, the inhibitory activity of complexes **1-3** is  $\sim 7$  times higher than that of cisplatin (28.5  $\mu\text{M}$ ). The results revealed that the compounds exhibited a severe cytotoxicity towards HepG2 cells, especially for the copper(II) complexes, indicating that synergy between the metal and ligands resulted in a significant enhancement in the cell death. The cytotoxicity induced by L might involve chelation of essential metals in all compartments of cells.<sup>44</sup> Although the exact molecular mechanism of cytotoxicity induced by copper(II) complexes is unclear, accumulating evidences point to the strong DNA binding involving hydrophobic forces of interaction and efficient DNA cleavage,<sup>45</sup> or the dissociation of the complexes in the cell resulting in the intracellular accumulation of high amounts of copper and the chelation with biological components such as protein out of nucleus.<sup>46</sup>

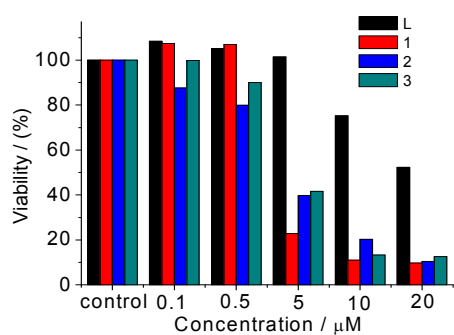


**Figure 12.** The viability of HepG2 cells upon treatment with L and the complexes for hours.

**Table 4.** Comparative IC50 Values of L and complexes **1-3** when tested on HepG2 Cell Lines after 24 h.

Compound	IC50 ( $\mu\text{M}$ )
L	21.2
<b>1</b>	3.6
<b>2</b>	3.9
<b>3</b>	4.2
[Pt(NH <sub>3</sub> ) <sub>2</sub> Cl <sub>2</sub> ]	28.5

## Conclusion

The ligand L (4-PDIP) and their three new copper(II) complexes have been synthesized and well characterized. The DNA binding properties of L and complexes **1-3** were examined by UV-Vis absorption spectra, emission spectra, viscosity, thermal melting, and unwinding assay, which suggested their involvement in intercalative DNA interaction with different binding affinities. While L (4-PDIP) intercalated with DNA through partially intercalating and the complexes **1-3** showed a higher affinity

toward CT-DNA than L. In the experiment of DNA cleavage, L and the complexes **1-3** showed cleavage activity with addition of H<sub>2</sub>O<sub>2</sub> as an activator. Active oxygen intermediates such as hydroxyl radicals and hydrogen peroxide may play an important role in the cleavage mechanism. The copper(II) center of complexes **1-3** may contribute to the significant DNA cleavage activity and high cytotoxicity to HepG2 cell lines.

## Author information

Corresponding Author  
\*E-mail: mjli@fzu.edu.cn. Fax: +86 591 22866135.  
yichq@mail.sysu.edu.cn.

## Acknowledgement

This work was supported by the National Scientific Foundation of China (NSFC No. 21171038, 31100723), the funding from Fuzhou University (No. 022309) and the Program for Changjiang Scholars and Innovative Research Team in University (No. IRT1116). Dr. Z. Wei in Xiamen University is acknowledged for the help in the crystallographic data collection. Beijing Institute of Research is acknowledged for access to the equipment for the crystal structural determination.

## Supporting Information Available

Measured and calculated isotope patterns of ligand and complexes. The cyclic voltammograms of complexes **2** and **3**, the unwinding assay for L complexes **1** and **2**, ethidium bromide stained agarose gel (1.0%) of pBR322 plasmid DNA (100 ng/ $\mu\text{L}$ ) in the presence of L and the complexes without the activators and X-ray crystallographic data in CIF format.

## References

- J. A. Cowan, *Curr. Opin. Chem. Biol.*, 2001, **5**, 634; C. -L. Liu, M. Wang, T. -L. Zhang and H. -Z. Sun, *Coord. Chem. Rev.*, 2004, **248**, 147.
- R. A. Kirgan, B. P. Sullivan and D. P. Rillema, *Top Curr Chem.*, 2007, **281**, 45.
- C. Yamamoto, H. Takemoto, K. Kuno, D. Yamamoto, A. Tsubura, K. Kamata, H. Hirata, A. Yamamoto, H. Kano, T. Seki and K. Inoue, *Hepatology*, 1999, **30**, 894.
- C. Metcalfe and J. A. Thomas, *Chem. Soc. Rev.*, 2003, **32**, 215; L. T.-L. Lo, W.-K. Chu, C.-Y. Tam, S.-M. Yiu, C.-C. Ko, and S.-K. Chiu, *Organometallics*, 2011, **30**, 5873.
- K. E. Erkkila, D. T. Odom, J. K. Barton, *Chem. Rev.*, 1999, **99**, 2777.
- J. K. Barton, *Science*, 1986, **233**, 727.
- B. Armitage, *Chem. Rev.*, 1998, **98**, 1171.
- D. R. McMillin and K. M. McNett, *Chem. Rev.*, 1998, **98**, 1201.
- M. Gonzalez-Alvarez, G. Alzuet, J. Borrás, M. Piti\_e and B. Meunier, *J. Biol. Inorg. Chem.*, 2003, **8**, 644.
- P. U. Maheswari, S. Roy, H. den Dulk, S. Barends, G. van Wezel, B. Kozlevcar, P. Gamez and J. Reedijk, *J. Am. Chem. Soc.*, 2006, **128**, 710.
- Y. An, M. -L. Tong, L. -N. Ji, Z. -W. Mao, *Dalton Trans.*, 2006, 2066.

- (12) S. Thyagarajan, N. N. Murthy, A. A. N. Sarjeant, K. D. Karlin and S. E. Rokita, *J. Am. Chem. Soc.*, 2006, **128**, 7003.
- (13) W. K. Pogozelski and T. D. Tullius, *Chem. Rev.*, 1998, **98**, 1089.
- (14) D. S. Sigman, A. Mazumder and D. M. Perrin, *Chem. Rev.*, 1993, **93**, 2295.
- (15) L. Pearson, C. B. Chen, R. P. Gaynor and D. S. Sigman, *Nucleic Acids Res.*, 1994, **22**, 2255.
- (16) T. Gupta, S. Dhar, M. Nethaji and A. R. Chakravarty, *Dalton Trans.*, 2004, 1896.
- (17) S. Dhar, P. A. N. Reddy and A. R. Chakravarty, *Dalton Trans.*, 2004, 697.
- (18) B. Selvakumar, V. Rajendiran, P. U. Maheshwari, H. Stoeckli-Evans and M. J. Palaniandavar, *Inorg. Biochem.*, 2006, **100**, 316; S. Dhar, M. Nethaji and A. R. Chakravarty, *Inorg. Chem.*, 2005, **44**, 8876; A. K. Patra, M. Nethaji and A. R. Chakravarty, *Dalton Trans.*, 2005, 2798.
- (19) K. J. Humphreys, K. D. Karlin and S. E. Rokita, *J. Am. Chem. Soc.*, 2002, **124**, 6009.
- (20) S. S. Bhat, A. A. Kumbhar, H. Heptullah, A. A. Khan, V. V. Gobre, S. P. Gejji and V. G. Puranik, *Inorg. Chem.*, 2011, **50**, 545.
- (21) S. I. Kirin, C. M. Happel, S. Hrubanova, T. Weyhermüller, C. Klein, N. Metzler-Nolte, *Dalton Trans.*, 2004, 1201.
- (22) K. J. Humphreys, K. D. Karlin and S. E. Rokita, *J. Am. Chem. Soc.*, 2002, **124**, 6009.
- (23) K. J. Humphreys, K. D. Karlin and S. E. Rokita, *J. Am. Chem. Soc.*, 2002, **124**, 8055.
- (24) M. Komiyama, S. Kina, K. Matsumura, J. Sumaoka, S. Tobey, V. M. Lynch and E. Anslyn, *J. Am. Chem. Soc.*, 2002, **124**, 13731; S. I. Kirin, C. M. Happel, S. Hrubanova, T. Weyhermüller, C. Klein and N. Metzler-Nolte, *Dalton Trans.*, 2004, 1201.
- (25) M. Yamada, Y. Tanaka, Y. Yoshimoto, S. Kuroda and I. Shimao, *Bull. Chem. Soc. Jpn.*, 1992, **65**, 1006.
- (26) Q. L. Zhang, J. H. Liu, X. Z. Ren, H. Xu, Y. Huang, J. Z. Liu and L. N. Ji, *J. Inorg. Biochem.*, 2003, **95**, 194.
- (27) Z. Otwinowski, W. Minor, *Macromol. Crystallogr., Pt A*, 1997, **276**, 307.
- (28) J. W. Chen, X. Y. Wang, Y. Shao, J. H. Zhu, Y. G. Zhu, Y. Z. Li, Q. Xu and Z. J. Guo, *Inorg. Chem.*, 2007, **46**, 3306.
- (29) M. Lee, A. L. Rhodes, M. D. Wyatt, S. Forrow and J. A. Hartley, *Biochemistry*, 1993, **32**, 4237.
- (30) J. Carmichael, W. G. Degraff, A. F. Gazdar, J. D. Minna, J. B. Mitchell, *Cancer Res.* 1987, **47**, 936-942.
- (31) V. Rajendiran, R. Karthik, M. Palaniandavar, H. S. Evans, V. S. Periasamay, M. A. Akbarsha, B. S. Srinag, H. Krishnamurthy, *Inorg. Chem.*, 2007, **46**, 8208.
- (32) A. Barve, A. Kumbhar, M. Bhat, B. Joshi, R. Butcher, U. Sonawane, R. Joshi, *Inorg. Chem.* 2009, **48**, 9120; G.-J. Chen., X. Qiao, P.-Q. Qiao, G.-J. Xu, J.-Y. Xu, J.-L. Tian, W. Gu, X. Liu, S.-P. Yan, *J. Inorg. Biochem.*, 2011, **105**, 119; B. Maity, M. Roy, B. Banik, R. Majumdar, R. R. Dighe, and A. R. Chakravarty, *Organometallics*, 2010, **29**, 3632.
- (33) T. Gupta, S. Dhar, M. Nethaji, A. Chakravarty, *Dalton Trans.*, 2004, 1896.
- (34) M. Baldini, M. Belicchi-Ferrari, F. Bisceglie, P. P. Dall'Aglio, G. Pelosi, S. Pinelli, P. Tarasconi, *Inorg. Chem.*, 2004, **43**, 7170.
- (35) E. Tselepi-Kalouli and N. Katsaros, *J. Inorg. Biochem.*, 1989, **37**, 271.
- (36) S. Satyanarayana, J. C. Dabrowiak and J. B. Chaires, *Biochemistry*, 1993, **32**, 2573.
- (37) P. Wittung, P. Nielsen and B. Norden, *J. Am. Chem. Soc.*, 1996, **118**, 7049.
- (38) J. Liu, T. Zhang, L. Qu, H. Zhou, Q. Zhang and J. Liangian, *J. Inorg. Biochem.*, 2002, **91**, 269.
- (39) P. Peixoto, C. Bailly, M. H. David-Cordonnier, *Methods Mol. Biol.* 2010, **613**, 235.
- (40) S. Mahadevan, M. Palaniandavar, *Inorg. Chem.*, 1998, **37**, 693; V. Rajendiran, M. Murali, E. Suresh, M. Palaniandavar, V. S. Periasamy, M. A. Akbarsha, *Dalton Trans.*, 2008, 2157.
- (41) W. C. Johnson, K. Nakanishi, N. Berova, R. W., Eds. Woody, *In Circular Dichroism: Principles and Applications*, VCH, New York, 1994, 523.
- (42) A. M. Nowicka, A. Kowalczyk, S. Sek, and Z. Stojek, *Anal. Chem.* 2013, **85**, 355; B. Ranjbar, P. Gill, *Chem. Biol. Drug Des.*, 2009, **74**, 101.
- (43) P. Uma Maheswari, M. Palaniandavar, *J. Inorg. Biochem.*, 2004, **98**, 219.
- (44) A. S. Johansson, M. Vestling, P. Zetterstrom, L. Lang, L. Leinartaitė, M. Karlstrom, J. Danielsson, S. L. Marklund, M. Oliveberg, *PLOS ONE*, DOI: 10.1371/journal.pone.0036104: e36104
- (45) S. S. Bhat, A. A. Kumbhar, H. Heptullah, A. A. Khan, V. V. Gobre, S. P. Gejji, V. G. Puranik, *Inorg. Chem.* 2011, **50**, 545; C. H. Ng, K. C. Kong, S. T. Von, P. Balraj, P. Jensen, E. Thirthagiri, H. Hamada, M. Chikira, *Dalton Trans.* 2008, 447; A. Barve, A. Kumbhar, M. Bhat, B. Joshi, R. Butcher, U. Sonawane, R. Joshi, *Inorg. Chem.* 2009, **48**, 9120; S. Zhang, Y. Zhu, C. Tu, H. Wei, Z. Yang, L. Lin, J. Ding, J. Zhang, Z. Guo, *J. Inorg. Biochem.*, 2004, **98**, 2099; V. Rajendiran, R. Karthik, M. Palaniandavar, H. S. Evans, V. S. Periasamay, M. A. Akbarsha, B. S. Srinag, H. Krishnamurthy, *Inorg. Chem.*, 2007, **46**, 8208; S. Ramakrishnan, V. Rajendiran, M. Palaniandavar, V. S. Periasamay, M. A. Akbarsha, B. S. Srinag, H. Krishnamurthy, *Inorg. Chem.*, 2009, **48**, 1309; R. Loganathan, S. Ramakrishnan, E. Suresh, A. Riyasdeen, M. A. Akbarsha, M. Palaniandavar, *Inorg. Chem.*, 2012, **51**, 5512.
- (46) S. Tardito, I. Bassanetti, C. Bignardi, L. Elviri, M. Tegoni, C. Mucchino, O. Bussolati, R. Franchi-Gazzola, L. Marchio, *J Am Chem Soc.* 2011, **133**, 6235.